

BALLASTLESS BRIDGE DECK FOR HSR

Polyakov, Vladimir Yu., Russian University of Transport, Moscow, Russia.
Dang, Ngok Tkhan, Russian University of Transport, Moscow, Russia / Nam Dinh, Vietnam.

ABSTRACT

The article is devoted to the study of oscillations of ballastless bridge deck, concrete slabs, conduct of rail fastenings, gasket layer under a rail slab of a high-speed railway. The objective of research

was to achieve reduction of forces in concrete slabs and rational stiffness of elastic elements in the structure of a carrying system, depending on load, speeds and features of the model «bridge–track–vehicle».

Keywords: railway, ballastless track, high-speed railway, bridge deck, dynamic studies, modeling, wheel, rail, vehicle, beam, span structure.

Background. The ballastless track superstructure is widely used on HSR, in China more than 80 % of high-speed railways are with concrete slabs [1]. In contrast to the traditional ballast one, a track with concrete slabs has many advantages, including maintaining geometric parameters for a long time and reducing maintenance costs [1–3]. However, in the zone of bridges and other artificial structures, it operates under specific conditions [4], caused by considerably greater deformations of an under-rail base due to fluctuations in span structures.

Most models used to study vibrations of bridges are focused on the study of dynamic conduct of a train or a span structure, less attention is paid to vibrations of a bridge, especially slabs thereon. This article discusses exactly fluctuations of slabs of a bridge deck, forces in intermediate rail fastenings, enveloping moments and shear forces in slabs, and at the same time influence of stiffness of a gasket layer under a rail slab to find an effective way to reduce forces in slabs and rational stiffness value of elastic elements.

Objective. The objective of the authors is to consider ballastless bridge deck for HSR.

Methods. The authors use general scientific and engineering methods, comparative analysis, modeling, graph construction, mathematical apparatus.

Results.

1. Model of a dynamic carrying system

1.1. Vehicle model

The need to consider joint fluctuations of cars, rails, under-rail slabs and span structure (i. e. carrying system [5]) requires development of a refined model. In it, a vehicle and a railway track are considered symmetrical with respect to the center line. Let's consider only vertical oscillations of a vehicle moving along the section. We assume the following assumptions [6]:

- 1. Bodies, bogies and wheels are not deformable.
- 2. Oscillations of bouncing and galloping are taken into account.

3. Coupling devices do not interfere with fluctuations.

4. A vehicle has a two-stage suspension.

5. Slabs of a ballastless track are located on a span structure or a roadbed, not overlapping a bridge and approach joint.

Such assumptions correspond to motion along a single-track span structure or to in-phase loading of two tracks, which is stipulated by special technical conditions for the design of HSR [7].

1.2. Differential equations

Equations of vehicle oscillations [8]:

[M]{Y¨(t)} + [C]{Y˙(t)} + [K]{Y(t)} = {F(t)} , (1)

where [M], [C] and [K] – matrix of mass, damping and stiffness of a vehicle, respectively; {Y(t)} and {F(t)} – displacement vector of a vehicle and dynamic load vector.

As shown in Pic. 1, moving forces of wheel-rail interaction, which are dependent on time Pn(t), and consisting of static Psta and dynamic forces Fwn(t) act on a rail as follows:

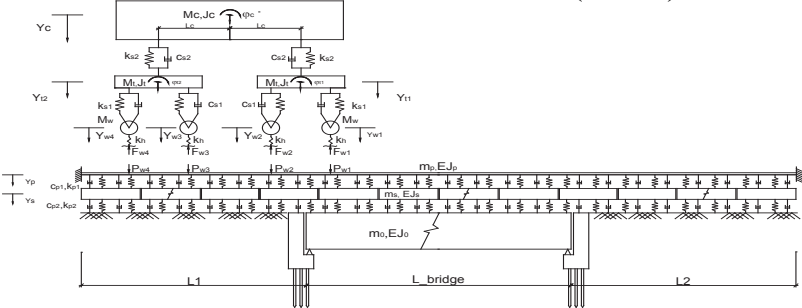
Pn(t) = Psta + Fwn(t) . (2)

The differential equations of oscillations of a rail, cars and a beam span structure, given in [9], are supplemented with the equations of oscillations of slabs of a ballastless track: on the approach

EsJs ∙ ∂4ys(x,t) / ∂x4 + ms ∙ ∂2ys(x,t) / ∂t2 + cp2 ∙ ∂ys / ∂t + kp2 ∙ ys = cp1 ∙ (∂yp / ∂t - ∂ys / ∂t) + kp1 ∙ (yp - ys); (3)

on the bridge

EsJs ∙ ∂4ys(x,t) / ∂x4 + ms ∙ ∂2ys(x,t) / ∂t2 + cp2 ∙ (∂ys / ∂t - ∂yk / ∂t) + kp2 ∙ (ys - yk) = cp1 ∙ (∂yp / ∂t - ∂ys / ∂t) + kp1 ∙ (yp - ys). (4)



Pic. 1. General model of a vehicle and a bridge.



Table 1

Critical speed of a train EVS-2 for a beam of 33,1 m

| $f_1, (1/c)$ | $V_{cr}, (km/h)$ | Model |
|--------------|------------------|--------------------|
| 4,60 | 410 | Core |
| 4,28 | 382 | Spatial model, MFE |

Table 2

Maximum deflections of a span structure at different speeds

| Speed of a train (km/h) | 340 | 360 | 380 | 400 | 410 |
|-------------------------------------|-------|-------|-------|-------|-------|
| Deflection of a span structure (mm) | 1,681 | 1,915 | 2,578 | 2,922 | 2,679 |

2. Design of a carrying system

In this ballastless structure of the track superstructure in the zone of a bridge crossing, upper slabs are laid on a lower slab of a deck, which is fastened to a beam of a span by outlets of reinforcement and connected to a beam by double-sided connections.

Various designs for connecting the upper and lower slabs of a ballastless track on a bridge and approaches were considered. A model with double-sided connections was used in the case of attaching the upper slab to the bottom (i. e. to a beam, since the lower slab is attached by means of outlets of reinforcement). A model with one-sided connections was used in the case of free support of the upper slab

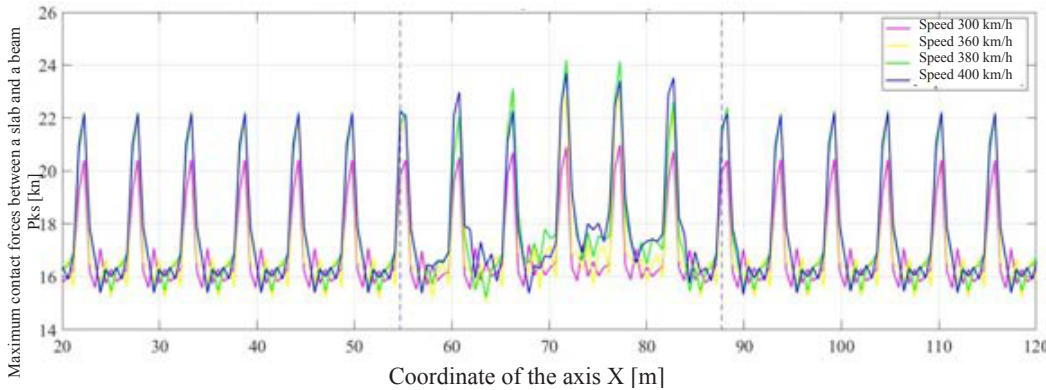
on the lower, foundation (i. e. beam). With the connections between a rail and a slab this corresponds to forces in intermediate fasteners. In the presence of forces between a slab and a beam, it is more correct to consider stresses, however, for convenience of comparing the results of different models, positive and negative (tearing off) forces are analyzed in the connections corresponding to the model in Pic. 1.

The span structure is a split beam with a design span of 33,1 m. The rolling stock is EVS-2 (10 cars), length of a car is 24,8 m.

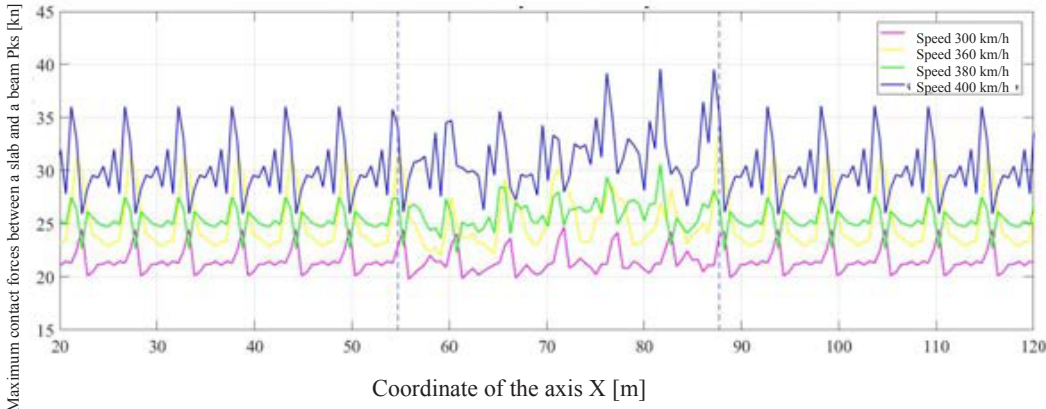
3.Numerical analysis

3.1. Critical speed of a train for a bridge

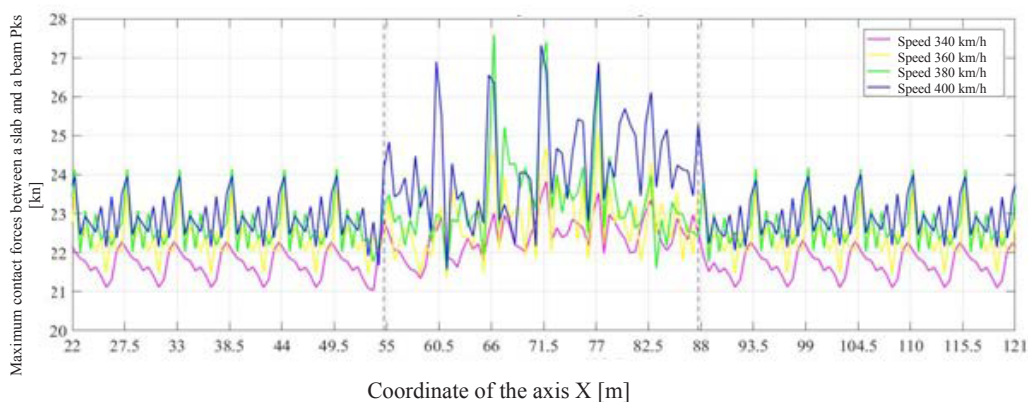
The critical speed corresponds to a frequency of oscillation excitation at which resonance is observed.



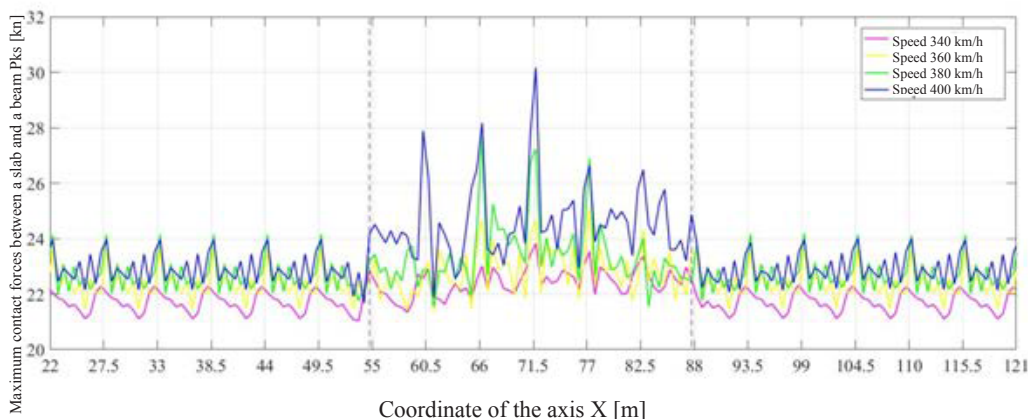
Pic. 2. Maximum contact forces between a slab and a beam with a stiffness coefficient of a gasket under a slab $3 \cdot 10^8$ N/m (double-sided).



Pic. 3. Maximum contact forces between a slab and a beam with a stiffness coefficient of a gasket under a slab $3 \cdot 10^9$ N/m (double-sided).



Pic. 4. Maximum contact forces between a slab and a beam in the absence of a layer (double-sided).



Pic. 5. Maximum contact forces between a slab and a beam in the absence of a layer (one-sided).

The natural oscillation frequency of a span structure can be determined as [10]:

$$f_i = \sqrt{\frac{EJ_0}{m_0} \cdot \frac{\pi \cdot i^2}{2L^2}}, \text{ where } i = 1, 2, 3, \dots \quad (5)$$

The resonance of a span structure occurs if $f_1 = f_{exc}$, where $f_{exc} = V/l_{car}$.

According to [11] the critical train speed for a bridge is $V_{cr} = f_1 \cdot l_{car}$.

The critical train speeds for a bridge are shown in Table 1, from which it can be seen that determination of natural frequencies of a beam span structure with the help of a spatial model of a box beam and a MFE differs from a beam core model by 7 %. The speeds from 300 km/h to the critical resonance are considered.

The maximum vertical displacements of a span structure with an estimated length of 33,1 m (core model) are shown in Table 2. At 400 km/h, near-resonance oscillations of a span structure are manifested. As can be seen, mass of a train and damping in its suspension make corrections to the natural frequencies of the system's oscillations and critical speed. For this model, a speed of 400 km/h is closer to resonance.

3.2. Load on plates and stiffness of a laying layer

Pic. 2–4 show envelope diagrams of load on the base of a top slab, i. e. maximum force in the model's

connections for entire time of passage of a 10-car train. The connections are double-sided, stiffness range of a layer is given in [12]. From comparison of the diagrams, it can be seen that a change in stiffness of a gasket layer does not lead to a monotonous change in the load on the base of a slab. When stiffness changes, the nature of the interaction changes, but in all cases the joints of slabs are noticeable. With minimal layer stiffness, concentration of forces in the joint zone is observed (increase in effort by 38 %), which is a condition for appearance of a risk. The greatest load is noted with stiffness of a connection of $3 \cdot 10^9$ N/m, which is 1,5 times greater than in the absence of a layer.

The soft layer between a slab and a base (Pic. 2, 3) makes a bridge virtually invisible in terms of load on the base slab. In the case of rigid support of a track slab, there is a noticeable increase in the load on the base over the entire speed range (by 11–12 %). It should be noted that accounting of the one-sided nature of the connections between a slab and its base does not introduce significant changes to the parameter in question, except for the case of rigid support: forces on a bridge and approaches differ by 25 % (Pic. 5), and the maxima for different connections differ by 11 % (Pic. 4, 5).

The contact forces in intermediate rail fastening (load from a rail to a slab) are practically independent of the nature of the connections between a slab and a base and stiffness of a slab contact with a base,



Table 3

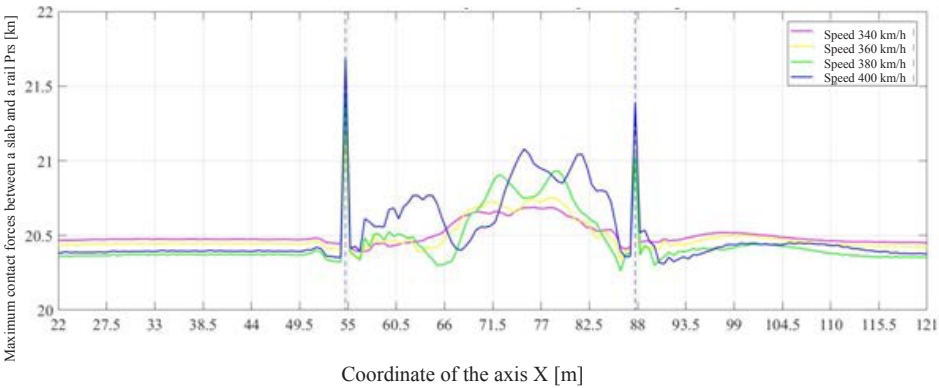
Tearing off relative movements of a slab and a beam with stiffness of a layer $3 \cdot 10^9$ N/m (one-sided)

| | | | | |
|------------------------|---------|---------|---------|---------|
| Train speed (km/h) | 300 | 360 | 380 | 400 |
| Slab displacement (mm) | -0,0040 | -0,0138 | -0,0218 | -0,0407 |

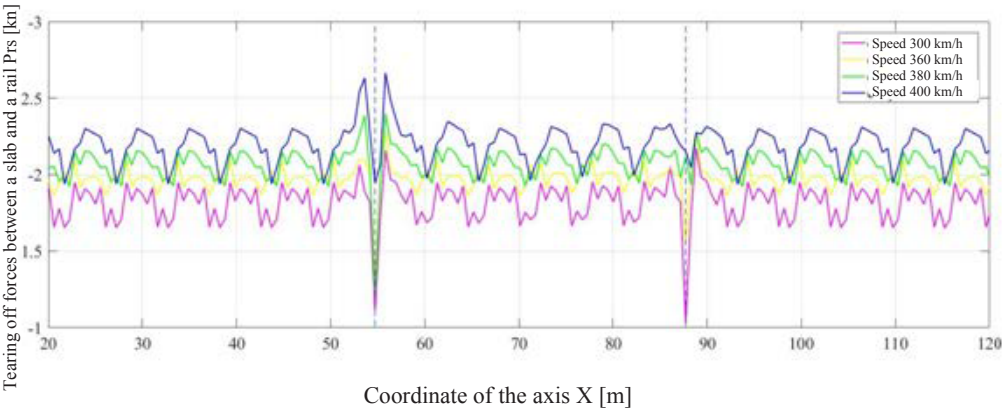
Table 4

Tearing off relative movements of a slab and a beam at different train speeds with stiffness of a gasket $3 \cdot 10^8$ N/m (one-sided)

| | | | | |
|------------------------|---------|---------|---------|---------|
| Train speed (km/h) | 300 | 360 | 380 | 400 |
| Slab displacement (mm) | -0,0126 | -0,0128 | -0,0154 | -0,0193 |



Pic. 6. Maximum contact forces between a slab and a rail in the absence of a layer (one-sided).



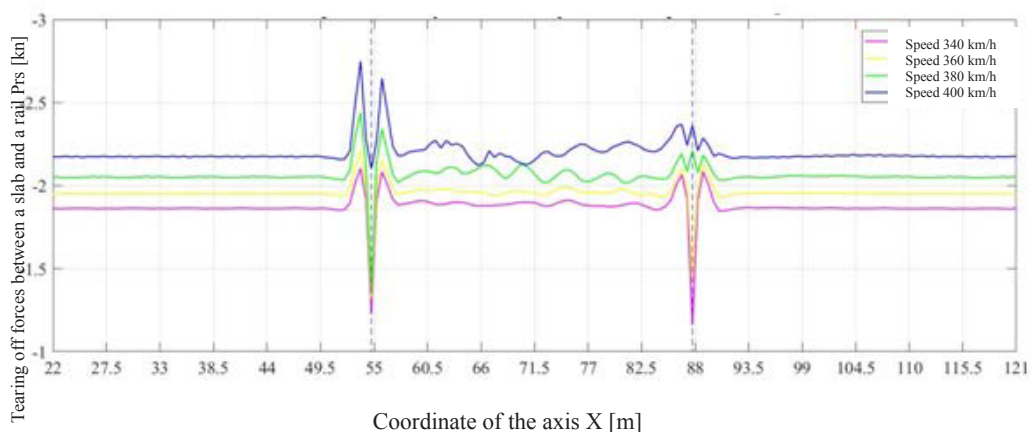
Pic. 7. Tearing off forces between a slab and a rail with a stiffness coefficient of a gasket under a slab $3 \cdot 10^8$ N/m (one-sided).

this effect remains relatively uniform along the length of the bridge zone. One can only note the growth of the load on the under-rail base in the second half of the span due to centrifugal acceleration of a vehicle (Pic. 6).

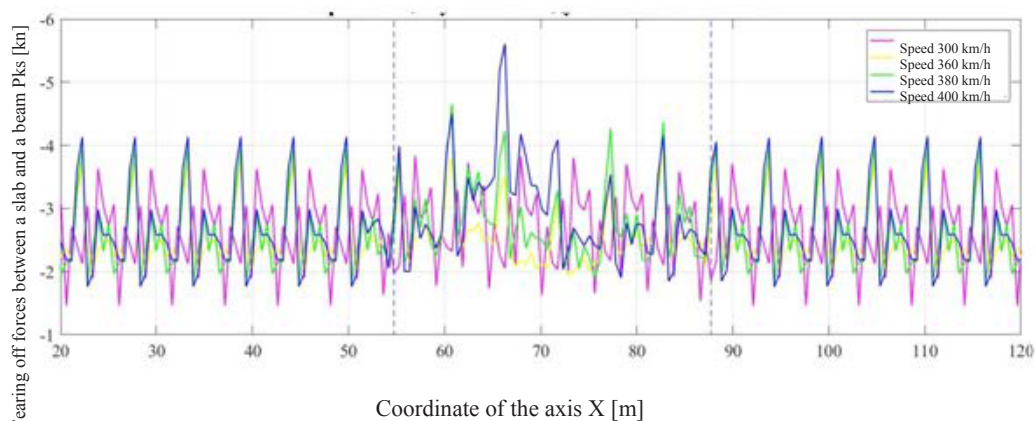
Attention is paid to efforts that can tear off a dowel in a slab or contribute to formation of cracks at the location of insert bolts (anchors). This effect is typical of intermediate rail fasteners, where the rail-to-plate connection is always double-sided. Pic. 7 shows enveloping maxima of tearing off forces in fasteners along the crossing length for a «soft» gasket layer and in its absence (Pic. 8). These two types of diagrams are also characteristic of other design options: with different types of connections and stiffness of layers. The diagrams differ little in

terms of the maximum values at the junctions of beams with approaches.

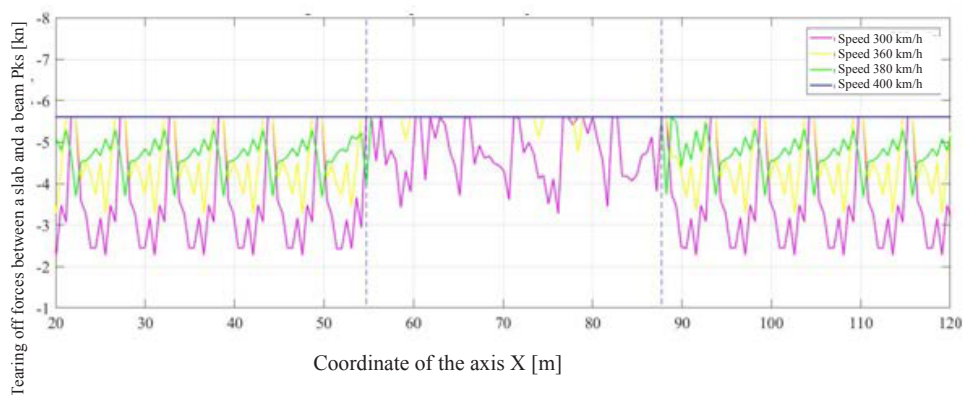
Of considerable interest are the «tearing off» forces between a slab and its base. If the connections here are double-sided, the physical nature of these forces is understandable. If the connections are one-sided, the presence of such a force means unloading the connection until the weight of a slab and a rail with a fastening is overcome. For a «soft» gasket layer (Pic. 9), the type of connection does not matter – one-sided connections do not appear, because the weight of a slab is not overcome. For a more rigid base slab, the diagrams of enveloping forces differ significantly for different connections (Pic. 10, 11). If, at a speed of 300 km/h, a slab breaks off from a base only in separate places (Pic. 10), then at higher speeds it is almost



Pic. 8. Tearing off forces between a slab and a rail in the absence of a gasket layer (one-sided).



Pic. 9. Tearing off contact forces between a slab and a beam with a stiffness coefficient of a gasket under a slab $3 \cdot 10^9$ N/m (one-sided and double-sided).

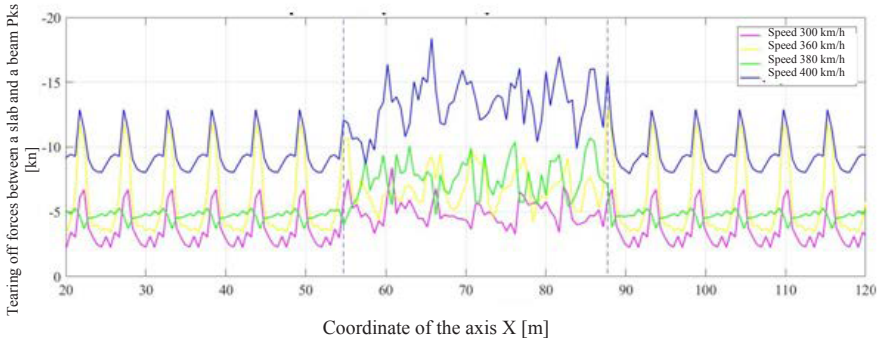


Pic. 10. Tearing off contact forces between a slab and a beam with a stiffness coefficient of a gasket under a slab $3 \cdot 10^9$ N/m (one-sided).

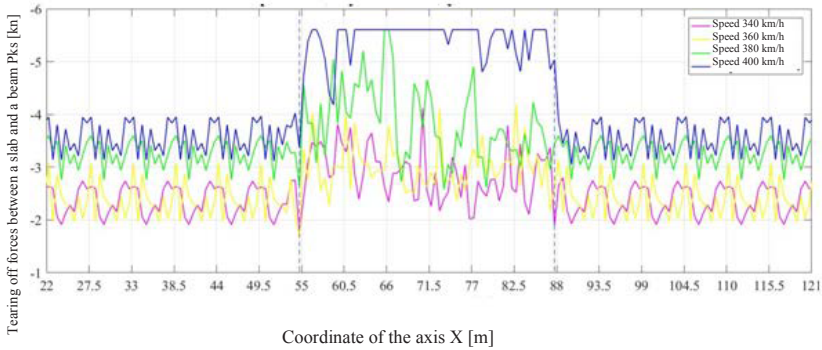
everywhere, and at a speed of 400 km/h – everywhere, including approaches to a roadbed. The amount of separation is limited by a rail, therefore it is small (Tables 3, 4) and, probably, does not pose a threat. Let's pay attention to the fact that at speed of 380 km/h plates on the approach do not break off, and this speed appears most favorable for a track on a roadbed.

In the design of a track superstructure with double-sided connections, the tearing off forces are comparable in absolute value with the maximum load (Pic. 3 and 11). Such features of dynamic conduct of a ballastless track superstructure in a bridge zone set a task of using reinforced slabs.

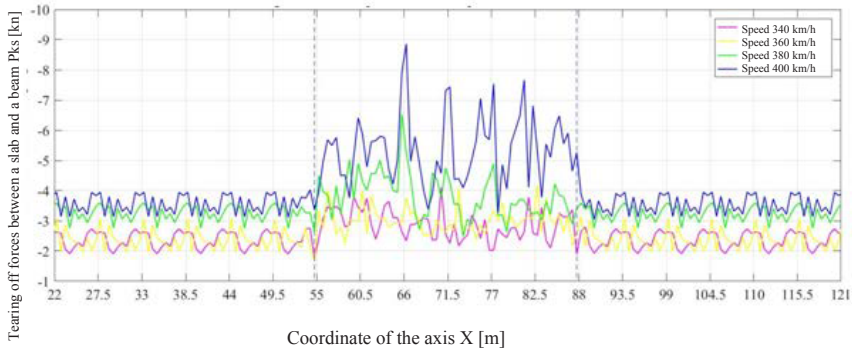




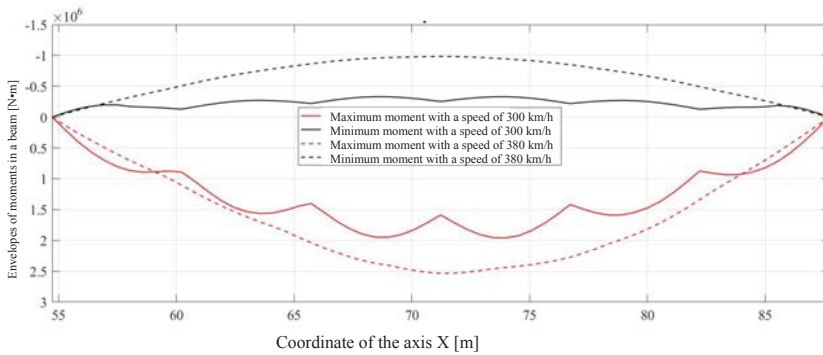
Pic. 11. Tearing off contact forces between a slab and a beam with a stiffness coefficient of a gasket under a slab $3 \cdot 10^9$ N/m (double-sided).



Pic. 12. Tearing off forces between a slab and a beam in the absence of a gasket layer (one-sided).



Pic. 13. Tearing off forces between a slab and a beam in the absence of a gasket layer (two-sided).



Pic. 14. Envelopes of moments in a beam. At a speed of 300 km/h, the contribution of the higher eigenmodes of oscillations is seen.

Table 5

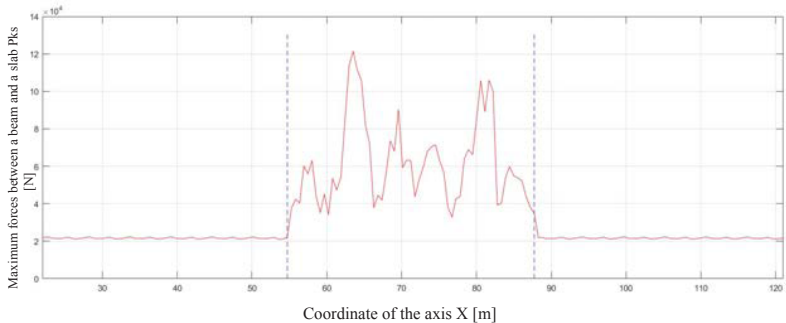
Maximum average stresses on a slab (Pa) (double-sided connections)

| | | | | |
|--|-------|-------|-------|-------|
| Train speed (km/h) | 300 | 360 | 380 | 400 |
| Stiffness of a gasket $3 \cdot 10^8$ N/m | 29354 | 32260 | 33826 | 33168 |
| Stiffness of a gasket $3 \cdot 10^9$ N/m | 34520 | 48156 | 42821 | 55357 |
| Without a gasket layer | 47014 | 35462 | 38592 | 38211 |

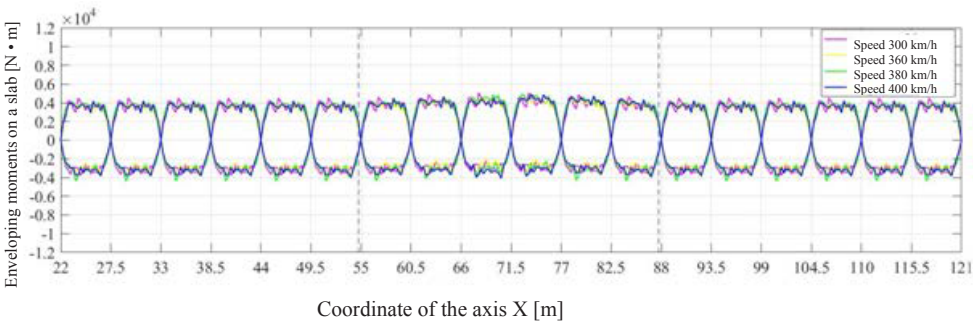
Table 6

Maximum average stresses on a slab (Pa) (one-sided connections)

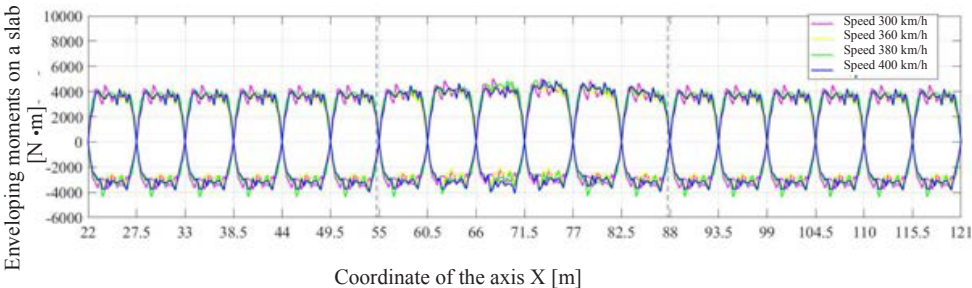
| | | | | |
|--|--------|-------|-------|-------|
| Train speed (km/h) | 300 | 360 | 380 | 400 |
| Stiffness of a gasket $3 \cdot 10^8$ N/m | 29354 | 32260 | 33826 | 33168 |
| Stiffness of a gasket $3 \cdot 10^9$ N/m | 34520 | 52980 | 81280 | 85662 |
| Without a gasket layer | 169831 | 35462 | 38667 | 42193 |



Pic. 15. Maximum contact forces between a slab and a beam in the absence of a layer at a speed of 300 km/h (one-sided).



Pic. 16. Envelope moments on a slab with a stiffness coefficient of a gasket under a slab $3 \cdot 10^9$ N/m (one-sided).



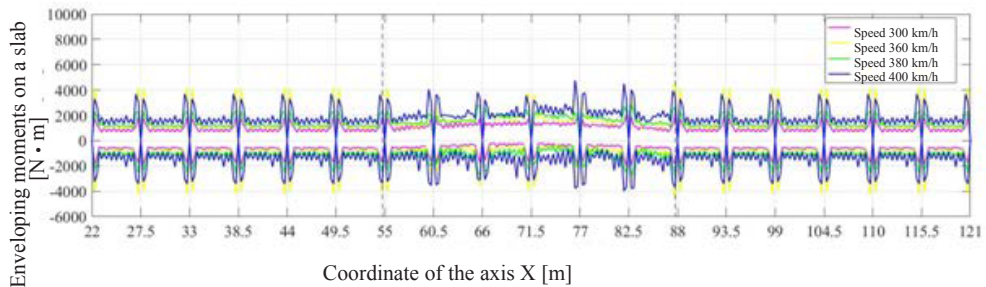
Pic. 17. The envelope moments on a slab with a stiffness coefficient of a gasket under a slab $3 \cdot 10^9$ N/m (double-sided).

Comparing the diagrams in Pic. 9, 11, 13 for double-sided connections, we note that stiffness $3 \cdot 10^9$ N/m is the worst for tearing off forces: a maximum is by two times higher than with a rigid support slab, and more than by 3 times – than with a «soft». For one-sided connections, stiffness does not

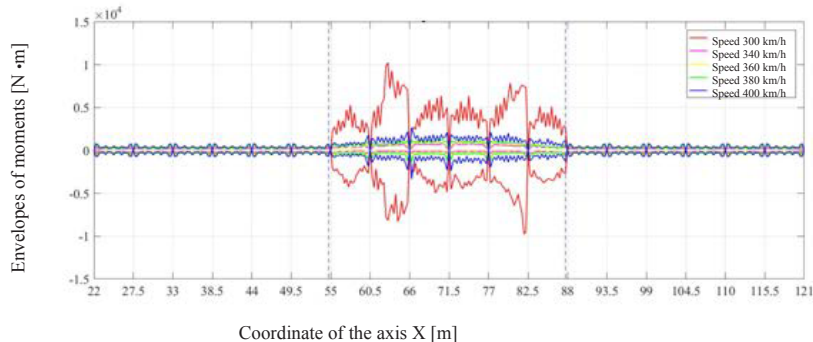
matter, since the limit of such forces in this case is weight of a slab (Tables 5, 6).

Separately, it is necessary to assess conduct of the system «bridge–track–vehicle» at a speed of 300 km/h. Table 6 shows that load on the lower slab (beam) is significantly different from other cases. At

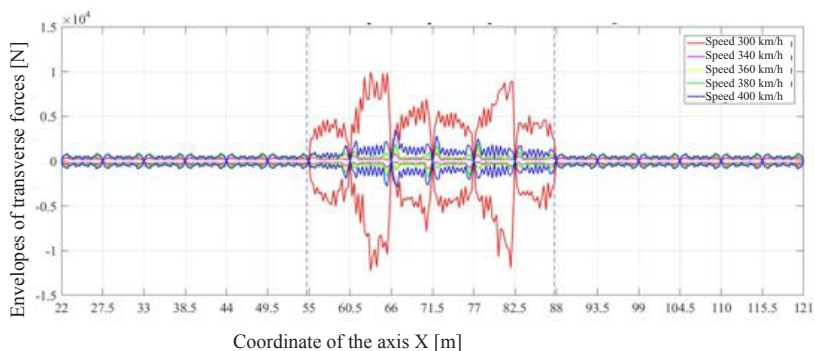




Pic. 18. The envelope moments in a slab with a stiffness coefficient of a gasket under a slab $3 \cdot 10^9$ N/m (double-sided).



Pic. 19. Envelopes of moments of a slab in the absence of a gasket layer (one-sided).



Pic. 20. Envelopes of transverse forces in a slab in the absence of a gasket layer (one-sided).

this speed, in the span polyharmonic oscillations with participation of the highest eigenforms are excited in the span structure. In Pic. 14 at a speed of 380 km/h, the maximum moments are formed mainly by the first form of natural oscillations with the maximum moment in the middle of the span (the moment index to one rail is shown). At a speed of 300 km/h, other eigenforms with a higher frequency of oscillations make a significant contribution. Essentially, waves of deformations propagate along a beam, which strongly affects conduct of slabs of a ballastless track. Pic. 15 shows the envelope of the stress diagram between a slab and a beam, where these forces exceed the maxima at other speeds (Pic. 5) fourfold. With double-sided connections between a slab and a beam, tearing off forces at a speed of 300 km/h increase by 90 % compared to other speeds (Pic. 13).

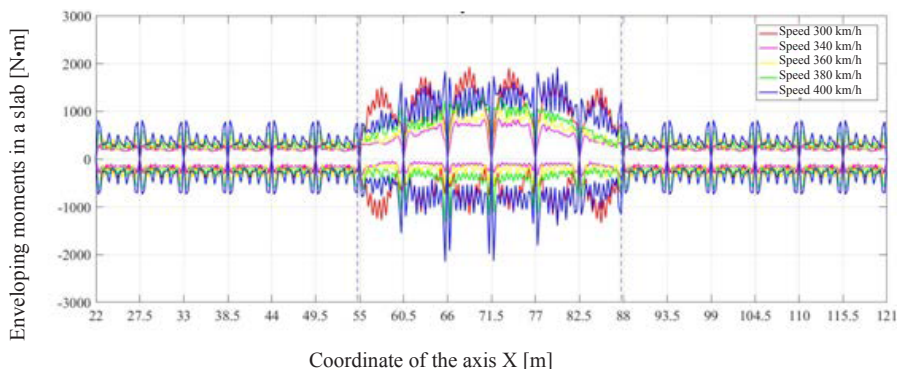
3.3. Internal forces in slabs

Internal forces in slabs are characterized by a bending moment and lateral force. The diagrams in this section show the envelope values of forces applied to one rail, along the length of the bridge zone.

It was revealed that the nature of the connection between a slab and a base does not exert a noticeable influence on the maximum bending moments and lateral forces in slabs of a ballastless track with minimum stiffness of a gasket layer (Pic. 16 and 17). With the maximum stiffness of a layer, the character of the envelopes changes, but the maxima remain the same (Pic. 18).

At a speed of 300 km/h, at which polyharmonic vibrations develop in a beam, bending moments in slabs of a track without a gasket layer increase by approximately 10 times to 10 kNm. Transverse forces also increase significantly (Pic. 20). The use of double-sided connections between a slab and a beam significantly reduces the force of such oscillations (Pic. 21).

Conclusion. First of all, it is necessary to draw a conclusion about the importance of consideration of HSR carrier system as a whole at high speeds, which allows for continuous interaction between its main elements – bridge, bridge deck and rolling stock. The model «bridge–track–vehicle» provides an opportunity



Pic. 21. Enveloping moments of a slab in the absence of a gasket layer (double-sided).

to describe the conduct of such a complex system and the interaction of its elements. Independent study and design of elements and related simplification of interaction, expressed in introduction of abstract concepts (equivalent load, reduced mass, etc.), leads to significant miscalculations. Owing to the application of the integrated approach, a significant influence of conduct of the span structure on the forces in the bridge deck has been revealed.

Internal forces in slabs of bridge ballastless deck in the absence of a gasket layer with polyharmonic oscillations of a beam significantly exceed the forces at other speeds. At the same time, attaching the slabs to a beam by double-sided connections seriously reduces the level of forces in polyharmonic oscillations. The presence of an elastic layer between the slabs of the ballastless track eliminates the problem for both one-sided and double-sided connections between the slab and the beam. Bilateral connections cause significant «tearing off» forces in them, which requires appropriate calculations.

The elastic layer in the form of mats between the slabs of a ballastless track (slab and beam) makes the bridge virtually invisible from the point of view of the load on the base of the under-rail plate. However, the presence of such a layer between the slabs on the embankment has a negative effect on the bending moments in the slabs. Therefore, it is advisable to use elastic mats between them only on the span structure.

REFERENCES

1. Xuhui He, Teng Wu, Yunfeng Zou, Y. Frank Chen, Hui Guo & Zhiwu Yu. Recent developments of high-speed railway bridges in China. *Structure and Infrastructure Engineering*, Vol. 13, 2017, Iss. 12, pp. 1584–1595.
2. Kolos, A. F., Kozlov, I. S. Modern constructions of track superstructure for construction of speed and high-speed rail lines [*Sovremennyye konstruksii verhnego stroeniya puti dlya stroitel'stva skorostnykh i vysokoskorostnykh zhelezнодорожных liniy*]. Byulleten' rezul'tatov nauchnykh issledovaniy, 2013, Iss. 1–2, pp. 16–21.
3. Savin, A. V. Choice of a design of a ballastless track [*Vybor konstruksii bezballastnogo puti*]. *Vestnik VNIIZhT*, 2014, Iss. 1, pp. 55–59.
4. Polyakov, V. Yu. On some features of the work of track superstructure on approaches to artificial structures [*O nekotorykh osobennostyakh raboty verhnego stroeniya puti na podhodakh k iskusstvennym sooruzheniyam*]. *Collection of scientific works of MIIT*, 1983, Iss. 739, pp. 103–107.
5. Polyakov, V. Yu. Interaction Optimization in Multibody Dynamic System, *International Journal of Theoretical and Applied Mechanics*, Vol. 2, 2017, pp. 43–51.
6. Polyakov, V. Yu. Interaction of rolling stock with elements of a bridge crossing in high-speed traffic. D.Sc. (Eng) thesis [*Vzaimodeistvie podvizhnogo sostava s elementami mostovogo perekhoda pri vysokoskorostnom dvizhenii*. *Dis. doc. tech. nauk*]. Moscow, 1994, 395 p.
7. STU. The artificial structures of the section Moscow–Kazan of Moscow–Kazan–Yekaterinburg high-speed railway. Technical standards and requirements for design and construction. Change No. 1 [*STU. Sooruzheniya iskusstvennye uchastka Moskva–Kazan vysokoskorostnoi magistrali Moskva–Kazan–Ekaterinburg. Tehnicheskie normy i trebovaniya k proektirovaniyu i stroitel'stvu*. *Izmenenie No. 1*]. St. Petersburg, 2016.
8. Polyakov, V. Yu., Dang Ngok Tkhan. Interaction of rolling stock and track in the bridge zone at HSR [*Vzaimodeistvie podvizhnogo sostava i puti v zone mostov na VSM*]. *Modern problems of design, construction and operation of a railway track: Proceedings of 14th international scientific-technical conference / RZD, MIIT*. Moscow, 2017, pp. 143–153.
9. Polyakov, V. Yu. Numerical simulation of interaction of rolling stock with bridge structures in high-speed traffic [*Chislennoe modelirovanie vzaimodeistviya podvizhnogo sostava s mostovymi konstruksiyami pri vysokoskorostnom dvizhenii*]. *Stroitel'naya mehanika i raschet sooruzhenii*, 2016, Iss. 2, pp. 54–60.
10. Frýba, L. Dynamic of railway bridges. Academia, Praha, 1996, 330 p.
11. Klasztorny, M., Podworna, M. Vertical vibrations of composite bridge/track structure/high-speed train systems. Part 1: Series-of-types of steel-concrete bridges. *Bulletin of the Polish academy of sciences technical sciences*, Vol. 62, No. 1, 2014, pp. 165–179.
12. Lei, Xiaoyan. High Speed Railway Track Dynamics. Models, Algorithms and Applications. Science Press, Beijing, 2017, 414 p.

Information about the authors:

Polyakov, Vladimir Yu. – D.Sc. (Eng), professor of the department of Bridges and Tunnels of Russian University of Transport, Moscow, Russia, pvy55@mail.ru.

Dang, Ngok Tkhan – Ph.D. student at the department of Bridges and Tunnels of Russian University of Transport, Moscow, Russia / Nam Dinh, Vietnam, dangthanh@mail.ru.

Article received 15.03.2018, accepted 27.04.2018.

